

# u-LLaVA: Unifying Multi-Modal Tasks via Large Language Model

Jinjin Xu, Liwu Xu, Yuzhe Yang, Xiang Li, Fanyi Wang, Yanchun Xie, Yi-Jie Huang, Yaqian Li \*  
OPPO Research Institute

## Abstract

Recent advancements in multi-modal large language models (MLLMs) have led to substantial improvements in visual understanding, primarily driven by sophisticated modality alignment strategies. However, predominant approaches prioritize global or regional comprehension, with less focus on fine-grained, pixel-level tasks. To address this gap, we introduce u-LLaVA, an innovative unifying multi-task framework that integrates pixel, regional, and global features to refine the perceptual faculties of MLLMs. We commence by leveraging an efficient modality alignment approach, harnessing both image and video datasets to bolster the model’s foundational understanding across diverse visual contexts. Subsequently, a joint instruction tuning method with task-specific projectors and decoders for end-to-end downstream training is presented. Furthermore, this work contributes a novel mask-based multi-task dataset comprising 277K samples, crafted to challenge and assess the fine-grained perception capabilities of MLLMs. The overall framework is simple, effective, and achieves state-of-the-art performance across multiple benchmarks. We also make our model, data, and code publicly accessible at <https://github.com/OPPOMLab/u-LLaVA>.

## 1. Introduction

Owing to the intrinsic difficulties associated with feature extraction in computer vision (CV) tasks, researchers have predominantly focused on perception rather than cognition over an extended duration. This emphasis bears a substantial impact on the development and understanding of various CV methodologies [22]. Although the development of deep neural networks and pre-training techniques has significantly reduced the difficulty of perception, it remains challenging to achieve homogeneity across downstream tasks due to substantial differences in their respective objectives. Recently, causal large language models such as GPT [5, 27, 28], Gemini [35] and LLaMA [36] have reached or come close to human-level performance on a variety of tasks. These advancements have also motivated re-

Table 1. Comparison of comprehension levels supported by existing MLLMs.

Methods	Image	Video	Region	Pixel
LLaVA [19]	✓	✗	✗	✗
MiniGPT-4 [56]	✓	✗	✗	✗
Video-LLaMA [52]	✓	✓	✗	✗
Video-ChatGPT [23]	✗	✓	✗	✗
Shikra [6]	✓	✗	✓	✗
CogVLM [40]	✓	✗	✓	✗
LISA [14]	✓	✗	✗	✓
u-LLaVA (ours)	✓	✓	✓	✓

searchers to incorporate LLMs as components [19, 56] or core elements [35, 40] in visual tasks, leading to the development of visual language models (VLMs), or multi-modal large language models (MLLMs). As a result, these methods have garnered increasing attention in recent times.

Typically, a multi-modal LLM consists of one or multiple encoders to extract features, paired with suitable mapping components (such as MLP [19], Q-Former[56], or cross-attention [2]), to align the other modalities with the textual domain. In comparison to the impressive performance of MLLMs on general-purpose understanding tasks, such as visual question answering (VQA), their capabilities in regional and pixel-level tasks are somewhat less remarkable [19, 56]. To achieve regional-level understanding, it is usual to convert target coordinates into tokens for causal language modeling, such as Shikra [6] and KOSMOS-2[26]. To further realize pixel-level understanding, mask-level decoders or extractors are introduced, such as LISA [14], Osprey [50] and Next-Chat [51]. However, such region comprehension requires extensive data for training, entailing high costs. Pixel-level understanding methods offer more flexibility, but entail introducing or designing specific segmentation modules.

In this paper, we propose u-LLaVA, a novel approach to enhance the general, region and even pixel-level comprehension abilities of MLLMs. To this end, we first design

\*Corresponding author

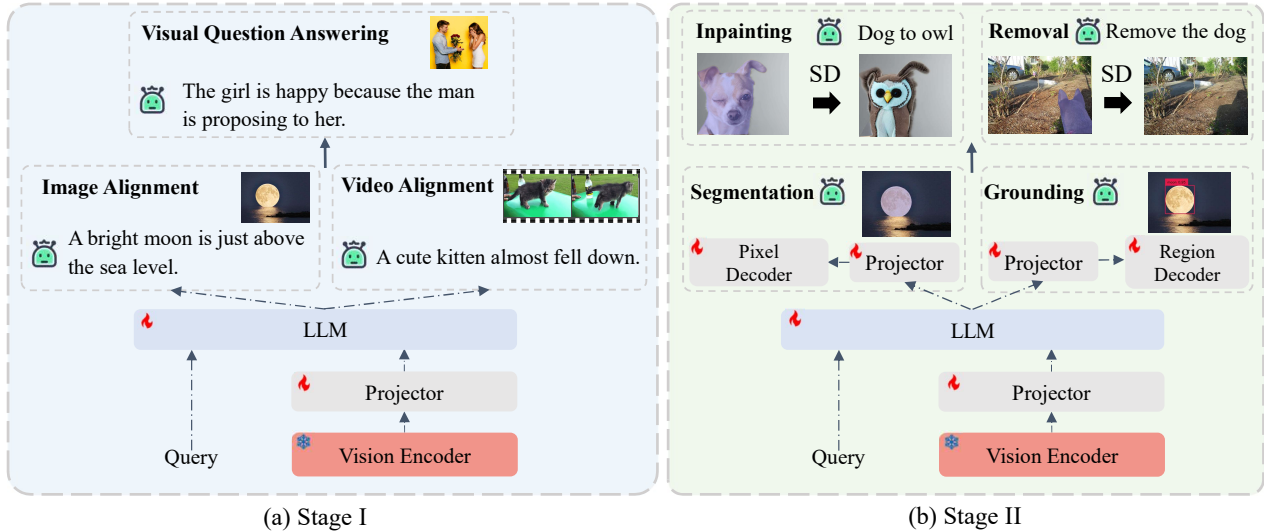


Figure 1. Overview of u-LLaVA. In stage I, image and spatio-temporal features are used to efficiently boost the general-purpose modality alignment. In Stage II, task-specific projectors and decoders are jointly trained for region and pixel-level understanding. Further, additional modules such as stable diffusion [31] can be easily patched for downstream tasks.

a efficient visual alignment strategy with image and spatio-temporal representations, and task-specific projectors and decoders are integrated for joint instruction tuning. The overall pipeline is illustrated in Figure 1.

To enable pixel-level understanding, we employ a projector to connect MLLMs and SAM [14], achieving two goals: a) imparting semantic understanding capacity to SAM by leveraging the world knowledge inherent in LLM; and b) enhancing the pixel-level understanding ability of LLM by harnessing SAM.

To enhance the performance of regional-level comprehension, we introduced an independent location decoder to decode target coordinates from the hidden state or output of MLLMs, which greatly reduces the amount of data required for training.

To accommodate the training of the aforementioned models, we have carefully designed a series of task-related prompt pools, and introduced a mask-based, region-specific dataset, namely ullava-277K. Most of the data was collected from publicly available datasets, with missing annotations carefully supplemented by the GPT-3.5.

Contributions can be summarized in three folds:

- We propose an efficient visual alignment method for multi-modal pre-training, which leverages image (spatio-temporal features) and video (spatio-temporal features) to enhance the perceptual faculties of MLLMs.
- We first-time introduce a joint instruction tuning approach in the same stage to enable multi-level understanding with task-specific projectors and decoders, see Table 1 for details.

- We release the joint instruction tuning dataset, ullava-277K, the model, and the code publicly available. Additionally, we conduct comprehensive experiments and demonstrate the effectiveness of the proposed method.

## 2. Related Work

### 2.1. MLLMs

Surprised by the remarkable abilities of large language models, researchers have shown great interest in transferring the capabilities of LLM to other domains [43, 48]. In recent months, remarkable progress has been made in this field, such as LLaVA [19], MiniGPT-4 [56], Otter [15], KOSMOS-1/2 [11, 26], mPLUG-owl [47] and Flamingo [1], etc. While having demonstrated impressive performance in image-level understanding, these methods show limited capabilities on pixel or region level tasks.

### 2.2. Region-Level Comprehension

Referring expression comprehension (REC) is one of the most typical region-level comprehension tasks, and RefCOCO [49], RefCOCO+ [49] and RefCOCOg [24], RefCLEF [12] are popular datasets for REC. Recently, some methods have employed the pix2seq approach to achieve regional understanding [6, 26]. Some strategies further incorporate regional encoding-decoding [51], while others utilize external modules to complete the task [53].

### 2.3. Pixel-Level Understanding

The advent of MLLMs has reduced the difficulty of subjective visual tasks, but progress on mask-aware tasks, such as referring expression segmentation (RES) and salient object segmentation, has been relatively slow due to the difficulty in designing pixel-level tokens. The prevalent methods currently involve using the output of grounding as the input for SAM [51], or utilizing a specific decoder for end-to-end training [14, 50].

## 3. Methods

The overall framework of u-LLaVA is presented in Figure 1. As we can see, u-LLaVA is a multi-modal multitask chatbot that takes text, images, and videos as inputs. It achieves this by unifying the representation space of visual and textual elements at stage I, and understanding region and pixel representations jointly at stage II. In this part, we will first introduce the model architecture and modality alignment strategy in Section 3.1, followed by a discussion on the joint instruction tuning process in Section 3.2. Lastly, we will present dataset construction methods.

### 3.1. Efficient Visual Alignment

To align representations among different modalities, the projector-based structure is adopted in this work: the pre-trained CLIP ViT-L/14 [29] and a visual projector are combined to encode image inputs, while the Vicuna [7] is employed as the cognitive module. In addition, u-LLaVA supports video modality by concatenating spatial and temporal representations, requiring only the addition of two special video tokens and a minimal amount of trainable parameters.

Table 2. Special tokens for modality and task expressions. Where  $T$  denotes the number of frames and is set 8 in this work.

	Image	Video	Tag	Region	Pixel
Begin	<img_beg>	<vid_beg>	<tag>	<LOC>	<SEG>
Patches	<img_patch>	<vid_patch>	/	/	/
End	</img_end>	</vid_end>	</tag>	/	/
Special token length	256	256+T	1	1	1

Generally, maximizing the likelihood function below to align the representation spaces of image/video and text is a widely-used approach for pre-training [19]. For a given image or video embeddings  $\mathbf{x}_e$ , and a conversation list of  $L$  tokens  $\mathbf{x}_t = \{x_t^1, x_t^2, \dots, x_t^L\}$ , we have the following training objectives, called *coarse-grained loss*:

$$L_{cgl} = \sum_i \log P(x_i | \mathbf{x}_e, x_{i-k}, \dots, x_{i-1}; \theta), \quad (1)$$

where, in accordance with [27],  $k$ ,  $P$ , and  $\theta$  are the size of context window, the conditional probability, and network parameters, respectively.

### 3.2. Joint Instruction Tuning

Visual instruction tuning is a common strategy for MLLM fine-tuning, but most methods only include one or two out of general, region, and pixel-level aspects during the training phase. In this work, we first-time jointly involve general, region, and pixel features in the same tuning stage.

**General-aware tuning:** In this part, there are no adjustments made to the model structure. However, unlike the first stage, we emphasize the use of multi-turn dialogues and complex reasoning datasets to further enhance the model’s understanding capabilities.

**Mask-aware tuning:** Inspired by LISA [14], we employ a projector to map the hidden states of the mask-related special tokens and then incorporate them into SAM decoder as the text embeddings to facilitate pixel-level understanding. We use a projector to connect SAM and MLLM, and map the mask-related hidden states as the text embedding for SAM. This endows SAM with semantic perception capabilities while achieving pixel-level perception for MLLM.

**Region-aware tuning:** Similar to pixel perception, we utilize a projector and a location decoder, mapping the hidden states of location-related special tokens directly to the target coordinates. In addition, we utilize the label information outputted by LLM as an input to the off-the-shelf region perception model, such as GroundingDINO [21], for redundant inference, thereby enhancing the accuracy of region perception.

In general, we have the following training objective, namely *fine-grained loss*:

$$L_{fgl} = L_{cgl} + \begin{cases} L_{pixel}, & \text{if mask exists} \\ L_{region}, & \text{if bbox exists} \\ 0, & \text{otherwise} \end{cases} \quad (2)$$

where the term  $L_{pixel} = \alpha_1 L_{bce} + \beta_1 L_{dice}$  represents the mask prediction loss, and  $L_{region} = \alpha_2 L_1 + \beta_2 L_{giou}$  is the prediction loss for the target bounding box. The values of  $\alpha_1$ ,  $\alpha_2$ ,  $\beta_1$ , and  $\beta_2$  are set to 2.0, 2.0, 0.5, and 1.0, respectively.

To this end, the special tokens used in this work are listed in Table 2.

### 3.3. Dataset Construction

To accommodate the training of the aforementioned models, we reorganize or rebuild various types of public datasets, details are summarized in Table 3.

As for the referring and semantic segmentation datasets, all references or semantic labels are extracted and then formed with the given templates. However, salient object

Table 3. Construction of the training datasets. The color blue indicates that the dataset is utilized in Stage I, while yellow signifies its usage in Stage II. Where annotations

	Dataset	Images/Videos	Annotations
Image Captioning	LLaVA CC3M 595K [19]	595,375	595,375
	Conversation-58K [19]	56,681	256,870
	Detail-23K [19]	23,240	23,240
Video Captioning	TGIF [17]	125,782	125,782
VQA	Complex-Reasoning-77K [19]	76,643	76,643
RES	RefCOCO [49]	16,994	120,624
	RefCOCO+ [49]	16,992	120,191
	RefCOCog [24]	21,899	80,512
	RefCLEF [12]	17,978	108,652
Semantic Segmentation	COCO-Stuff [29]	118,205	742,787
	VOC2010 [8]	4,366	81,139
	PACO-LVIS [30]	45,790	612,188
	ADE20K [54]	20,196	165,120
Salient-15K	MSRA-10K [9]	10,000	10,000
	MSRA-B [37]	5,000	5,000

detection/segmentation datasets usually lack descriptions of the target objects. To address this issue, we employ mask information to extract the primary objects from images within MSRA-10K [9] and MSRA-B [37]. The extracted objects are then fed into BLIP2 [16] to generate descriptions solely for the objects. Lastly, GPT3.5 is used to phrase the object tags from the generated description, followed by the integration of predefined templates to complete the reconstruction process. We refer to the reconstructed salient instruction dataset as Salient-15K for short. The template examples and construction process of Salient-15K are summarized in Appendix.

## 4. Experiments

### 4.1. Implementation Details

All experiments are conducted with 8 NVIDIA Tesla A100 80G GPUs and Pytorch framework [25]. Vicuna v1.1 [7] and CLIP ViT-L/14 [29] are set to the foundational language model and image encoder. SAM ViT-H [13] is selected as the mask decoder. A three-layer MLP with channels of [4096, 2048, 4] and GroundingDINO Swin-T OGC [21] are set to the region decoders for hidden states and tags, respectively. The vision projector for representation alignment and the hidden state projector for segmentation are two MLPs with channels of [1024, 4096] and [256, 4096, 4096]. We select AdamW optimizer with the weight decay of 0, and learning rates of  $2e-3$  and  $2e-5$  for the first and the second stages (if LoRA [10] used in the Stage II, the learning rate will be set to  $2e-4$ ). The batch size per device is set to 32 and 16 (48 if LoRA) with gradient accumulation step of 1 for the two stages. The first stage of training takes

approximately 4 hours for 1 epoch, while the second stage of training takes around 33 hours (20 hours if LoRA) for 5 epochs.

### 4.2. Evaluation Metrics

We follow the previous works [14, 18] to validate the quantitative performance of the proposed algorithm, with specific details as follows:

**Pixel Segmentation:** Cumulative-IoU (cIoU) is a widely-used performance indicator in segmentation tasks, which calculates the total intersection pixels over the total union pixels. In some works, it is also referred to as the overall-IoU (oIoU), as seen in [44, 46].

**Region Grounding:** The percentage of samples with IoU higher than a threshold  $X$  is a commonly used metric in visual grounding tasks, denoted as Precision@ $X$  (Prec@ $X$ ). In this work, we set the threshold to 0.5 according to [6].

### 4.3. Pixel-Level Understanding Performance

To demonstrate the performance of the proposed method on pixel-level understanding, we conduct experiments on widely-used RES benchmarks, RefCOCO, RefCOCO+, and RefCOCog. The comparison is made between existing state-of-the-art (SOTA) specialist models and MLLMs with cIoU indicator, as presented in Table 4.

As can be seen from the table, even with LoRA, our method still achieves the best results among the MLLMs methods. More notably, u-LLaVA-7B surpasses the performance of the prevailing state-of-the-art MLLM method, LISA-7B\*(ft), achieving an average improvement of 5.84. It is also noteworthy that u-LLaVA either matches or surpasses the performance of the current leading expert model, UNINEXT(H) [44], on the three benchmarks, all while utilizing merely a tenth of the training data. These findings serve as a testament to the efficacy of LLM in tasks that necessitate comprehension-based capabilities.

### 4.4. Pixel-level Intent Understanding Performance

We further examine the zero-shot performance of u-LLaVA in widely recognized salient segmentation datasets to clarify the superiority of MLLMs in comprehending human subjective intentions.

Here, DUT-OMRON [45] (5,168 test images), DUTS-TE [38] (5,019 test images), and ECSSD [32] (1000 test images) datasets are selected for validation. To ensure fairness, we draw parallels between our method and a range of other previously conducted unsupervised algorithms. As summarized in Table 5, u-LLaVA outperforms the rest, achieving SOTA performance across all three benchmarks, further solidifying the effectiveness and superiority of our method.

Table 4. RES results with cIoU indicator. Specialists represent models that are specifically designed for CV tasks. Where \* in MLLMs denotes using LoRA [10] for parameter efficient training. The top 2 results are outlined in **bold** and with underline.

Type	Method	Segmentation Masks	RefCOCO			RefCOCO+			RefCOCOg	
			val	test A	test B	val	test A	test B	val	test
Specialists	LAVT [46]	0.03M	72.73	75.82	68.79	62.14	68.38	55.10	61.24	62.09
	X-Decoder(L) [57]	0.12M	-	-	-	-	-	-	64.60	-
	ReLA [18]	-	73.82	76.48	70.18	66.04	71.02	57.65	65.00	65.97
	SEEM(B) [58]	0.12M	-	-	-	-	-	-	65.00	-
	SEEM(L) [58]	0.12M	-	-	-	-	-	-	65.60	-
	PolyFormer(B) [20]	0.16M	74.82	76.64	71.06	67.64	72.89	59.33	67.76	69.05
	PolyFormer(L) [20]	0.16M	75.96	78.29	73.25	69.33	74.56	61.87	69.20	70.19
	UNINEXT(L) [44]	3M	<u>80.32</u>	<u>82.61</u>	<u>77.76</u>	<u>70.04</u>	<u>74.91</u>	<u>62.57</u>	<u>73.41</u>	<u>73.68</u>
	UNINEXT(H) [44]	3M	<b>82.19</b>	<b>83.44</b>	<b>81.33</b>	<b>72.47</b>	<b>76.42</b>	<b>66.22</b>	<b>74.67</b>	<b>76.37</b>
MLLMs	LISA-7B* [14]	~ 0.80M	74.10	76.50	71.10	62.40	67.40	56.50	66.40	68.50
	LISA-7B* (ft) [14]	-	74.90	79.10	72.30	65.10	70.80	58.10	67.90	70.60
	NExT-Chat-7B [51]	0.15M	74.70	78.90	69.50	65.10	71.90	56.70	67.00	67.00
	u-LLaVA-7B* (Ours)	~ 0.66M	<u>78.70</u>	<u>81.46</u>	<u>75.97</u>	<u>68.95</u>	<u>73.19</u>	<u>62.26</u>	<u>71.57</u>	<u>72.91</u>
	u-LLaVA-7B (Ours)	~ 0.66M	<b>80.29</b>	<b>82.81</b>	<b>77.40</b>	<b>72.61</b>	<b>75.96</b>	<b>67.14</b>	<b>74.07</b>	<b>75.20</b>

Table 5. Salient segmentation results on salient object detection benchmarks among different methods, where † denotes the method with Bilateral solver[3], and cIoU is adopted as the metric.

Type	Method	DUT-OMRON	DUTS-TE	ECSSD
Specialists	LOST† [34]	48.90	57.20	72.30
	TokenCut† [42]	61.80	62.40	77.20
	SELFMASK† [33]	<b>65.50</b>	66.60	<b>81.80</b>
	MOVE † [4]	<u>63.60</u>	<b>68.70</b>	<u>80.10</u>
MLLMs	u-LLaVA-7B* (Ours)	<b>72.14</b>	<u>72.35</u>	<u>87.11</u>
	u-LLaVA-7B (Ours)	<u>71.64</u>	<b>74.23</b>	<b>89.73</b>

#### 4.5. Region-Level Understanding Performance

In this section, we conduct a comparative analysis to evaluate u-LLaVA’s performance against other 7B MLLM models in the context of region-level understanding tasks, using the REC task as the benchmark.

It should be highlighted that we incorporate all intermediate results of our model, including the output of the region decoder, the mask, and the grounding results based on tags, to generate the final regression box thus optimizing the performance. This comprehensive process is visually encapsulated in Figure 3, and the corresponding experimental results are summarized in Table 6. Observably, u-LLaVA exhibits results closely paralleling those of Shikra [6], while utilizing a mere one-tenth of the data, and outperforms other models in the RefCOCO testB and RefCOCOg subsets. While there exists a discernible performance gap when compared to expert models such as UNINEXT(H), it is essential to consider that this is influenced by multi-

ple factors, including but not limited to input resolution and task interference.

#### 4.6. Dataset Ablation

As shown in Table 7, we validate the impact of employing varied types of datasets during the second stage of the model’s training on its overall performance. The results indicate that embracing diversity in dataset types fosters improved generalization of the algorithm, thereby circumventing the potential risk of overfitting on specific tasks. In essence, the algorithm’s robustness is enhanced with an increased variety of dataset types.

#### 4.7. Qualitative examples

Qualitative comparison with existing multi-task MLLM methods, LISA [14], Shikra [6] and CogVLM [40], on grounding and segmentation tasks are given in Figure 2. More illustrations can be found in Appendix.

### 5. Conclusions

In this work, we introduce u-LLaVA, a multi-modal large language model that jointly tunes instructions at the global, regional, and pixel levels. Through innovative structural design and data configuration, we have achieved optimal performance in various comprehension-based tasks.

Currently, the pre-training and task adaptation of MLLMs remain an open area with many directions yet to be explored. This study represents an exploratory and experimental effort building upon previous works such as LLaVA and LISA. We believe that the open-sourcing of our work can provide valuable assistance to the development of this field.



Table 6. Comparative experiments of existing 7B MLLM models on REC tasks with Prec@0.5 indicator. The top 2 results are outlined in **bold** and with underline.

Type	Method	Grounding Boxes	RefCOCO			RefCOCO+			RefCOCOg	
			val	test A	test B	val	test A	test B	val	test
Specialists	SeqTR [55]	1.5M	87.00	90.15	83.59	78.69	84.51	71.87	82.69	83.37
	GroundingDINO(L) [21]	-	90.56	93.19	88.24	82.75	88.95	75.92	86.13	87.02
	OFA [39]	-	<u>92.04</u>	<u>94.03</u>	88.44	<b>87.86</b>	<b>91.70</b>	<b>80.71</b>	<u>88.07</u>	88.78
	UNINEXT(L) [44]	3M	91.43	93.73	<u>88.93</u>	83.09	87.90	76.15	86.91	87.48
	UNINEXT(H) [44]	3M	<b>92.64</b>	<b>94.33</b>	<b>91.46</b>	<u>85.24</u>	<u>89.63</u>	<u>79.79</u>	<b>88.73</b>	<b>89.37</b>
MLLMs	Shikra-7B [6]	~ 4M	<b>87.01</b>	<b>90.61</b>	80.24	<b>81.60</b>	<b>87.36</b>	<b>72.12</b>	<b>82.27</b>	<u>82.19</u>
	VisonLLM-H-7B [41]	0.15M	-	86.70	-	-	-	-	-	-
	NeXT-Chat-7B [51]	~ 4M	85.50	90.00	77.90	<u>77.20</u>	<u>84.50</u>	68.00	80.10	79.80
	u-LLaVA-7B* (Ours)	0.39M	84.51	88.25	79.81	72.71	79.43	63.02	79.52	79.77
	u-LLaVA-7B (Ours)	0.39M	<u>86.15</u>	<u>90.28</u>	<b>81.14</b>	76.16	82.94	<u>68.37</u>	<u>81.31</u>	<b>82.61</b>

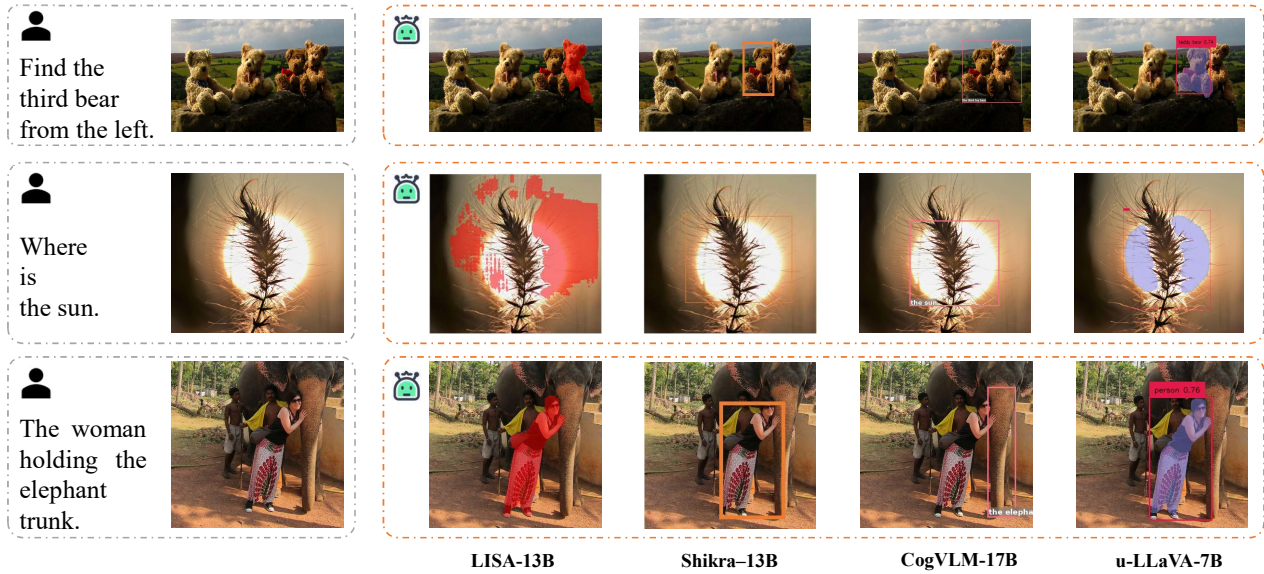


Figure 2. Qualitative examples of existing methods for regional and pixel-level understanding.

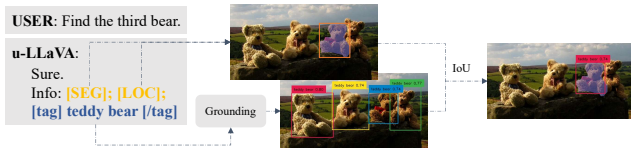


Figure 3. The inference workflow of u-LLaVA for region-level comprehension tasks.

Table 7. Ablations on the Stage II training datasets, where “LoRA” and “Full” indicate whether LoRA strategy is employed, and cIoU is used as the performance indicator.

Exp.	Referring	Semantic	Salient	Captioning	RefCOCOg test		DUT-OMRON	
					LoRA	Full	LoRA	Full
1	✓				71.26	72.83	52.77	52.04
2	✓	✓			72.55	75.04	53.57	46.70
3	✓	✓		✓	72.11	74.33	46.46	42.04
4	✓	✓	✓		72.26	75.10	66.47	65.45
5	✓	✓	✓	✓	<b>72.91</b>	<b>75.20</b>	<b>72.14</b>	<b>71.64</b>

## 6. Acknowledgements

This work is sponsored by Shanghai Pujiang Program (23PJ1421800).

# u-LLaVA: Unifying Multi-Modal Tasks via Large Language Model

## Supplementary Material

### 7. Appendix

#### 7.1. Templates

Here, we present examples of task templates used by u-LLaVA on different type of training data.

##### Template examples for salient segmentation task

```
<image> What makes the image stand out?  
<image> What is salient one in this image?  
<image> Look at the image, segment the main  
object in the picture and explain.
```

##### Template examples for video captioning task

```
<video> Describe the video concisely.  
<video> What's happening in this video?  
<video> Write a terse but informative summary  
of the VCR.
```

##### Template examples for RES task

```
<image> Segment out the <class>.  
<image> Output the mask of the <class>.  
<image> Find the <class> in the picture.
```

#### 7.2. Construction of Salient-15K

As shown in Figure 4, given that the MSRA-10K and MSRA-B datasets are devoid of label information and image descriptions pertaining to the principal subjects, we initially proceed by extracting the subjects from the images and subsequently inputting them into BLIP2 [16] for a rudimentary description. Following this, we employ GPT3.5 to parse the target labels emanating from the elementary description, thereby enabling an expansion of the description information. This approach facilitates a more comprehensive understanding of the subjects within the datasets while compensating for the initial lack of descriptive data.

#### 7.3. Conversations with u-LLaVA

Examples on VQA, video understanding and inpainting are presented in Figure 5. Besides, we show results of complex reasoning in Fig. 6, and video captioning results in Fig. 7. We also illustrate the object removal and inpainting results in Fig. 8.

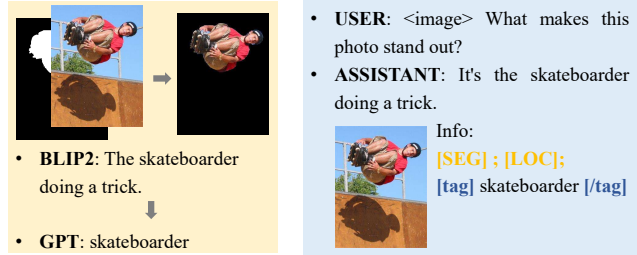


Figure 4. The process workflow of Salient-15K.

### References

- [1] Jean-Baptiste Alayrac, Jeff Donahue, Pauline Luc, Antoine Miech, Iain Barr, Yana Hasson, Karel Lenc, Arthur Mensch, Katherine Millican, Malcolm Reynolds, et al. Flamingo: a visual language model for few-shot learning. *Advances in Neural Information Processing Systems*, 35:23716–23736, 2022. 2
- [2] Jinze Bai, Shuai Bai, Shusheng Yang, Shijie Wang, Sinan Tan, Peng Wang, Junyang Lin, Chang Zhou, and Jingren Zhou. Qwen-vl: A versatile vision-language model for understanding, localization, text reading, and beyond. 2023. 1
- [3] Jonathan T Barron and Ben Poole. The fast bilateral solver. In *European conference on computer vision*, pages 617–632. Springer, 2016. 5
- [4] Adam Bielski and Paolo Favaro. Move: Unsupervised movable object segmentation and detection. *Advances in Neural Information Processing Systems*, 35:33371–33386, 2022. 5
- [5] Tom Brown, Benjamin Mann, Nick Ryder, Melanie Subbiah, Jared D Kaplan, Prafulla Dhariwal, Arvind Neelakantan, Pranav Shyam, Girish Sastry, Amanda Askell, et al. Language models are few-shot learners. *Advances in neural information processing systems*, 33:1877–1901, 2020. 1
- [6] Keqin Chen, Zhao Zhang, Weili Zeng, Richong Zhang, Feng Zhu, and Rui Zhao. Shikra: Unleashing multimodal llm’s referential dialogue magic. *arXiv preprint arXiv:2306.15195*, 2023. 1, 2, 4, 5, 6
- [7] Wei-Lin Chiang, Zhuohan Li, Zi Lin, Ying Sheng, Zhanghao Wu, Hao Zhang, Lianmin Zheng, Siyuan Zhuang, Yonghao Zhuang, Joseph E. Gonzalez, Ion Stoica, and Eric P. Xing. Vicuna: An open-source chatbot impressing gpt-4 with 90%\* chatgpt quality, 2023. 3, 4
- [8] Mark Everingham, Luc Van Gool, Christopher KI Williams, John Winn, and Andrew Zisserman. The pascal visual object classes (voc) challenge. *International journal of computer vision*, 88:303–338, 2010. 4
- [9] Qibin Hou, Ming-Ming Cheng, Xiaowei Hu, Ali Borji,

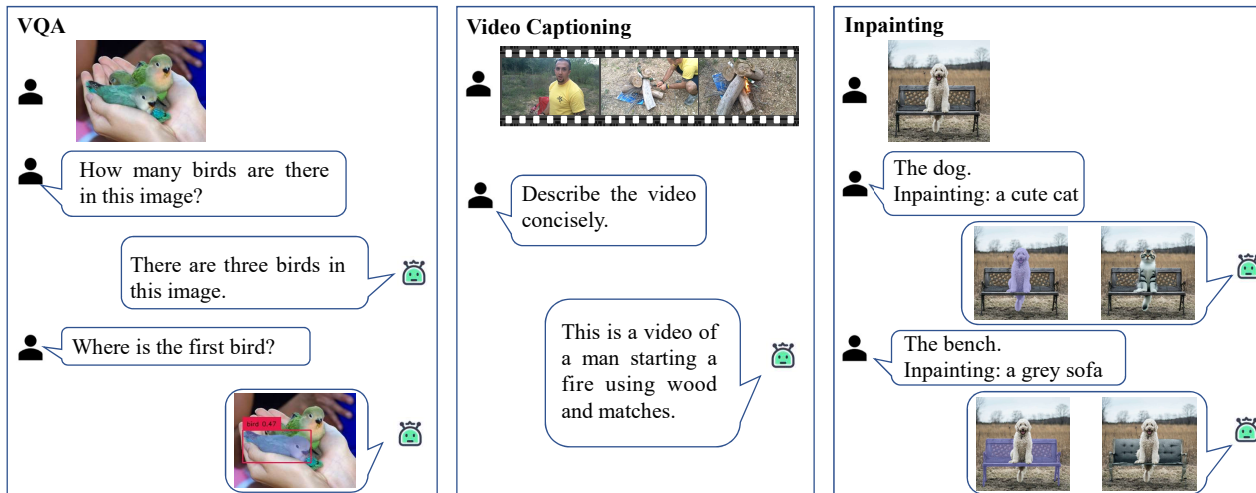


Figure 5. VQA, video captioning and inpainting examples.

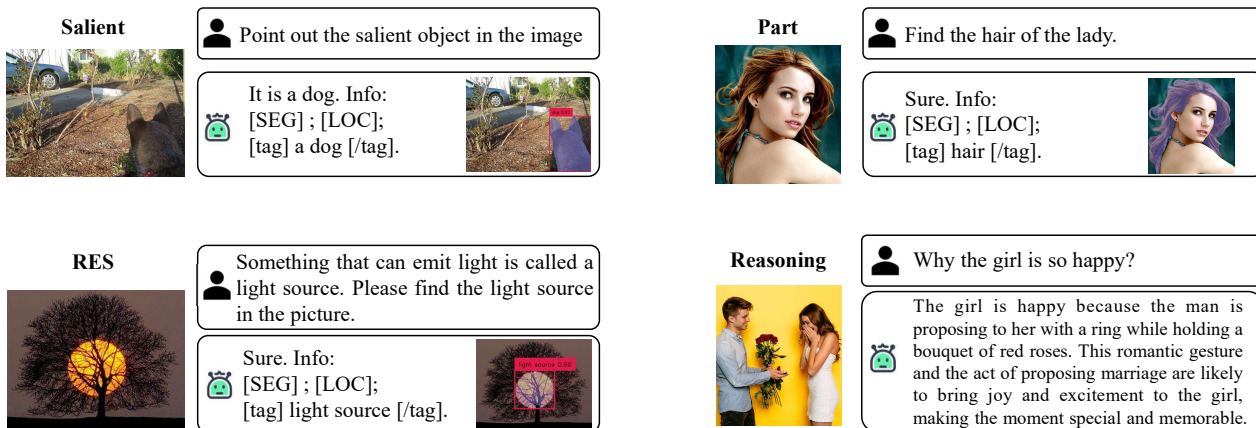


Figure 6. Conversation examples with u-LLaVA-7B.

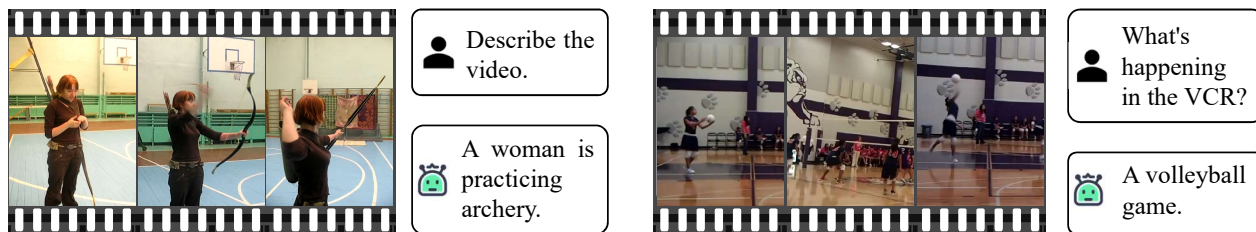


Figure 7. Video captioning examples with u-LLaVA-7B.

Zhuowen Tu, and Philip Torr. Deeply supervised salient object detection with short connections. *IEEE TPAMI*, 41(4): 815–828, 2019. 4

[10] Edward J Hu, Yelong Shen, Phillip Wallis, Zeyuan Allen-

Zhu, Yuanzhi Li, Shean Wang, Lu Wang, and Weizhu Chen. Lora: Low-rank adaptation of large language models. *arXiv preprint arXiv:2106.09685*, 2021. 4, 5

[11] Shaohan Huang, Li Dong, Wenhui Wang, Yaru Hao,





Figure 8. Image inpainting and object removal examples with u-LLaVA-7B.

- Saksham Singhal, Shuming Ma, Tengchao Lv, Lei Cui, Owais Khan Mohammed, Qiang Liu, et al. Language is not all you need: Aligning perception with language models. *arXiv preprint arXiv:2302.14045*, 2023. 2
- [12] Sahar Kazemzadeh, Vicente Ordonez, Mark Matten, and Tamara Berg. Referitgame: Referring to objects in photographs of natural scenes. In *Proceedings of the 2014 conference on empirical methods in natural language processing (EMNLP)*, pages 787–798, 2014. 2, 4
- [13] Alexander Kirillov, Eric Mintun, Nikhila Ravi, Hanzi Mao, Chloe Rolland, Laura Gustafson, Tete Xiao, Spencer Whitehead, Alexander C Berg, Wan-Yen Lo, et al. Segment anything. *arXiv preprint arXiv:2304.02643*, 2023. 4
- [14] Xin Lai, Zhuotao Tian, Yukang Chen, Yanwei Li, Yuhui Yuan, Shu Liu, and Jiaya Jia. Lisa: Reasoning segmentation via large language model. *arXiv preprint arXiv:2308.00692*, 2023. 1, 2, 3, 4, 5
- [15] Bo Li, Yuanhan Zhang, Liangyu Chen, Jinghao Wang, Jingkang Yang, and Ziwei Liu. Otter: A multi-modal model with in-context instruction tuning. *arXiv preprint arXiv:2305.03726*, 2023. 2
- [16] Junnan Li, Dongxu Li, Silvio Savarese, and Steven Hoi. Blip-2: Bootstrapping language-image pre-training with frozen image encoders and large language models. *arXiv preprint arXiv:2301.12597*, 2023. 4, 1
- [17] Yuncheng Li, Yale Song, Liangliang Cao, Joel Tetreault, Larry Goldberg, Alejandro Jaimes, and Jiebo Luo. Tgif: A new dataset and benchmark on animated gif description. In *Proceedings of the IEEE Conference on Computer Vision and Pattern Recognition*, pages 4641–4650, 2016. 4
- [18] Chang Liu, Henghui Ding, and Xudong Jiang. Gres: Generalized referring expression segmentation. In *Proceedings of the IEEE/CVF Conference on Computer Vision and Pattern Recognition (CVPR)*, pages 23592–23601, 2023. 4, 5
- [19] Haotian Liu, Chunyuan Li, Qingyang Wu, and Yong Jae Lee. Visual instruction tuning. *arXiv preprint arXiv:2304.08485*, 2023. 1, 2, 3, 4
- [20] Jiang Liu, Hui Ding, Zhaowei Cai, Yuting Zhang, Ravi Kumar Satzoda, Vijay Mahadevan, and R. Manmatha. Polyformer: Referring image segmentation as sequential polygon generation. In *Proceedings of the IEEE/CVF Conference on Computer Vision and Pattern Recognition (CVPR)*, pages 18653–18663, 2023. 5
- [21] Shilong Liu, Zhaoyang Zeng, Tianhe Ren, Feng Li, Hao Zhang, Jie Yang, Chunyuan Li, Jianwei Yang, Hang Su, Jun Zhu, et al. Grounding dino: Marrying dino with grounded pre-training for open-set object detection. *arXiv preprint arXiv:2303.05499*, 2023. 3, 4, 6
- [22] David G Lowe. Distinctive image features from scale-invariant keypoints. *International journal of computer vision*, 60:91–110, 2004. 1
- [23] Muhammad Maaz, Hanoona Rasheed, Salman Khan, and Fahad Shahbaz Khan. Video-chatgpt: Towards detailed video understanding via large vision and language models. *arXiv preprint arXiv:2306.05424*, 2023. 1
- [24] Junhua Mao, Jonathan Huang, Alexander Toshev, Oana Camburu, Alan L Yuille, and Kevin Murphy. Generation and comprehension of unambiguous object descriptions. In *Proceedings of the IEEE conference on computer vision and pattern recognition*, pages 11–20, 2016. 2, 4
- [25] Adam Paszke, Sam Gross, Francisco Massa, Adam Lerer, James Bradbury, Gregory Chanan, Trevor Killeen, Zeming Lin, Natalia Gimelshein, Luca Antiga, Alban Desmaison, Andreas Kopf, Edward Yang, Zachary DeVito, Martin Raison, Alykhan Tejani, Sasank Chilamkurthy, Benoit Steiner, Lu Fang, Junjie Bai, and Soumith Chintala. Pytorch: An imperative style, high-performance deep learning library. In *Advances in Neural Information Processing Systems 32*, pages 8024–8035. Curran Associates, Inc., 2019. 4
- [26] Zhiliang Peng, Wenhui Wang, Li Dong, Yaru Hao, Shaohan Huang, Shuming Ma, and Furu Wei. Kosmos-2: Grounding multimodal large language models to the world. *arXiv preprint arXiv:2306.14824*, 2023. 1, 2
- [27] Alec Radford, Karthik Narasimhan, Tim Salimans, Ilya Sutskever, et al. Improving language understanding by generative pre-training. *OpenAI blog*, 2018. 1, 3
- [28] Alec Radford, Jeffrey Wu, Rewon Child, David Luan, Dario Amodei, Ilya Sutskever, et al. Language models are unsupervised multitask learners. *OpenAI blog*, 1(8):9, 2019. 1
- [29] Alec Radford, Jong Wook Kim, Chris Hallacy, Aditya Ramesh, Gabriel Goh, Sandhini Agarwal, Girish Sastry, Amanda Askell, Pamela Mishkin, Jack Clark, et al. Learning transferable visual models from natural language supervision. In *International conference on machine learning*, pages 8748–8763. PMLR, 2021. 3, 4
- [30] Vignesh Ramanathan, Anmol Kalia, Vladan Petrovic, Yi Wen, Baixue Zheng, Baishan Guo, Rui Wang, Aaron Marquez, Rama Kovvuri, Abhishek Kadian, et al. Paco: Parts and attributes of common objects. In *Proceedings of the IEEE/CVF Conference on Computer Vision and Pattern Recognition*, pages 7141–7151, 2023. 4
- [31] Robin Rombach, Andreas Blattmann, Dominik Lorenz,

- Patrick Esser, and Björn Ommer. High-resolution image synthesis with latent diffusion models, 2021. 2
- [32] Jianping Shi, Qiong Yan, Li Xu, and Jiaya Jia. Hierarchical image saliency detection on extended cssd. *IEEE transactions on pattern analysis and machine intelligence*, 38(4): 717–729, 2015. 4
- [33] Gyungin Shin, Samuel Albanie, and Weidi Xie. Unsupervised salient object detection with spectral cluster voting. In *Proceedings of the IEEE/CVF Conference on Computer Vision and Pattern Recognition*, pages 3971–3980, 2022. 5
- [34] Oriane Siméoni, Gilles Puy, Huy V Vo, Simon Roburin, Spyros Gidaris, Andrei Bursuc, Patrick Pérez, Renaud Marlet, and Jean Ponce. Localizing objects with self-supervised transformers and no labels. *arXiv preprint arXiv:2109.14279*, 2021. 5
- [35] Gemini Team, Rohan Anil, Sebastian Borgeaud, Yonghui Wu, Jean-Baptiste Alayrac, Jiahui Yu, Radu Soricut, Johan Schalkwyk, Andrew M Dai, Anja Hauth, et al. Gemini: a family of highly capable multimodal models. *arXiv preprint arXiv:2312.11805*, 2023. 1
- [36] Hugo Touvron, Thibaut Lavril, Gautier Izacard, Xavier Martinet, Marie-Anne Lachaux, Timothée Lacroix, Baptiste Rozière, Naman Goyal, Eric Hambro, Faisal Azhar, et al. Llama: Open and efficient foundation language models. *arXiv preprint arXiv:2302.13971*, 2023. 1
- [37] Jingdong Wang, Huaizu Jiang, Zejian Yuan, Ming-Ming Cheng, Xiaowei Hu, and Nanning Zheng. Salient object detection: A discriminative regional feature integration approach. *International Journal of Computer Vision*, 123(2): 251–268, 2017. 4
- [38] Lijun Wang, Huchuan Lu, Yifan Wang, Mengyang Feng, Dong Wang, Baocai Yin, and Xiang Ruan. Learning to detect salient objects with image-level supervision. In *Proceedings of the IEEE conference on computer vision and pattern recognition*, pages 136–145, 2017. 4
- [39] Peng Wang, An Yang, Rui Men, Junyang Lin, Shuai Bai, Zhikang Li, Jianxin Ma, Chang Zhou, Jingren Zhou, and Hongxia Yang. Ofa: Unifying architectures, tasks, and modalities through a simple sequence-to-sequence learning framework. In *International Conference on Machine Learning*, pages 23318–23340. PMLR, 2022. 6
- [40] Weihang Wang, Qingsong Lv, Wenmeng Yu, Wenyi Hong, Yan Wang, Junhui Ji, Zhuiyi Yang, Lei Zhao, Xixuan Song, Jiazheng Xu, Xu Bin, Huanzi Li, Yuxiao Dong, Ming Ding, and Jie Tang. Cogvlm: Visual expert for large language models. *arXiv preprint*, 2023. 1, 5
- [41] Wenhai Wang, Zhe Chen, Xiaokang Chen, Jiannan Wu, Xizhou Zhu, Gang Zeng, Ping Luo, Tong Lu, Jie Zhou, Yu Qiao, et al. VisionLlm: Large language model is also an open-ended decoder for vision-centric tasks. *Advances in Neural Information Processing Systems*, 36, 2024. 6
- [42] Yangtao Wang, Xi Shen, Shell Xu Hu, Yuan Yuan, James L Crowley, and Dominique Vaufreydaz. Self-supervised transformers for unsupervised object discovery using normalized cut. In *Proceedings of the IEEE/CVF Conference on Computer Vision and Pattern Recognition*, pages 14543–14553, 2022. 5
- [43] Shengqiong Wu, Hao Fei, Leigang Qu, Wei Ji, and Tat-Seng Chua. Next-gpt: Any-to-any multimodal llm. *arXiv preprint arXiv:2309.05519*, 2023. 2
- [44] Bin Yan, Yi Jiang, Jiannan Wu, Dong Wang, Ping Luo, Zehuan Yuan, and Huchuan Lu. Universal instance perception as object discovery and retrieval. In *Proceedings of the IEEE/CVF Conference on Computer Vision and Pattern Recognition (CVPR)*, pages 15325–15336, 2023. 4, 5, 6
- [45] Chuan Yang, Lihe Zhang, Huchuan Lu, Xiang Ruan, and Ming-Hsuan Yang. Saliency detection via graph-based manifold ranking. In *Proceedings of the IEEE conference on computer vision and pattern recognition*, pages 3166–3173, 2013. 4
- [46] Zhao Yang, Jiaqi Wang, Yansong Tang, Kai Chen, Hengshuang Zhao, and Philip H.S. Torr. Lavt: Language-aware vision transformer for referring image segmentation. In *Proceedings of the IEEE/CVF Conference on Computer Vision and Pattern Recognition (CVPR)*, pages 18155–18165, 2022. 4, 5
- [47] Qinghao Ye, Haiyang Xu, Guohai Xu, Jiabo Ye, Ming Yan, Yiyang Zhou, Junyang Wang, Anwen Hu, Pengcheng Shi, Yaya Shi, et al. mplug-owl: Modularization empowers large language models with multimodality. *arXiv preprint arXiv:2304.14178*, 2023. 2
- [48] Shukang Yin, Chaoyou Fu, Sirui Zhao, Ke Li, Xing Sun, Tong Xu, and Enhong Chen. A survey on multimodal large language models. *arXiv preprint arXiv:2306.13549*, 2023. 2
- [49] Licheng Yu, Patrick Poirson, Shan Yang, Alexander C Berg, and Tamara L Berg. Modeling context in referring expressions. In *Computer Vision—ECCV 2016: 14th European Conference, Amsterdam, The Netherlands, October 11–14, 2016, Proceedings, Part II 14*, pages 69–85. Springer, 2016. 2, 4
- [50] Yuqian Yuan, Wentong Li, Jian Liu, Dongqi Tang, Xinjie Luo, Chi Qin, Lei Zhang, and Jianke Zhu. Osprey: Pixel understanding with visual instruction tuning. *arXiv preprint arXiv:2312.10032*, 2023. 1, 3
- [51] Ao Zhang, Liming Zhao, Chen-Wei Xie, Yun Zheng, Wei Ji, and Tat-Seng Chua. Next-chat: An lmm for chat, detection and segmentation. *arXiv preprint arXiv:2311.04498*, 2023. 1, 2, 3, 5, 6
- [52] Hang Zhang, Xin Li, and Lidong Bing. Video-llama: An instruction-tuned audio-visual language model for video understanding. *arXiv preprint arXiv:2306.02858*, 2023. 1
- [53] Yang Zhao, Zhijie Lin, Daquan Zhou, Zilong Huang, Jiashi Feng, and Bingyi Kang. Bubogpt: Enabling visual grounding in multi-modal llms. *arXiv preprint arXiv:2307.08581*, 2023. 2
- [54] Bolei Zhou, Hang Zhao, Xavier Puig, Sanja Fidler, Adela Barriuso, and Antonio Torralba. Scene parsing through ade20k dataset. In *Proceedings of the IEEE conference on computer vision and pattern recognition*, pages 633–641, 2017. 4
- [55] Chaoyang Zhu, Yiyi Zhou, Yunhang Shen, Gen Luo, Xingjia Pan, Mingbao Lin, Chao Chen, Liujuan Cao, Xiaoshuai Sun, and Rongrong Ji. Seqtr: A simple yet universal network for visual grounding. In *European Conference on Computer Vision*, pages 598–615. Springer, 2022. 6

- [56] Deyao Zhu, Jun Chen, Xiaoqian Shen, Xiang Li, and Mohamed Elhoseiny. Minigt-4: Enhancing vision-language understanding with advanced large language models. *arXiv preprint arXiv:2304.10592*, 2023. 1, 2
- [57] Xueyan Zou, Zi-Yi Dou, Jianwei Yang, Zhe Gan, Linjie Li, Chunyuan Li, Xiyang Dai, Harkirat Behl, Jianfeng Wang, Lu Yuan, Nanyun Peng, Lijuan Wang, Yong Jae Lee, and Jianfeng Gao. Generalized decoding for pixel, image, and language. In *Proceedings of the IEEE/CVF Conference on Computer Vision and Pattern Recognition (CVPR)*, pages 15116–15127, 2023. 5
- [58] Xueyan Zou, Jianwei Yang, Hao Zhang, Feng Li, Linjie Li, Jianfeng Gao, and Yong Jae Lee. Segment everything everywhere all at once. *arXiv preprint arXiv:2304.06718*, 2023. 5